

# Aggregation behavior of quaternary salt based cationic surfactants

Jitendra Mata<sup>a,\*</sup>, Dharmesh Varade<sup>a</sup>, Prashant Bahadur<sup>b</sup>

<sup>a</sup> Department of Chemistry, South Gujarat University, Surat 395007, India

<sup>b</sup> Department of Chemical Engineering, Sarvajani College of Engineering & Technology, Surat 395001, India

Received 25 May 2004; received in revised form 16 September 2004; accepted 1 November 2004

Available online 13 December 2004

## Abstract

The aggregation behavior of pure cationic surfactants (quaternary salts) in water has been studied by electrical conductivity (at 293.15–333.15 K), surface tension, dye solubilization and viscosity measurements (at 303.15 K). Critical micelle concentrations (CMCs), degree of counter ion dissociation ( $\beta$ ), aggregation number and sphere-to-rod transition for cationic surfactants are reported. Using law of mass action model, the thermodynamic parameters, viz. Gibbs energy ( $\Delta G_m^\circ$ ), enthalpy ( $\Delta H_m^\circ$ ) and entropy ( $\Delta S_m^\circ$ ) were evaluated. The plots of differential conductivity,  $(dk/dc)_{T,P}$ , versus the total surfactant concentration enables us to determine the CMC values more precisely than the conventional method. Surfactants with longer hydrocarbon chain are adapted to rodlike micelle better than to a spherical micelle. The data are explained in terms of molecular characteristics of surfactants viz. nonpolar chain length, polar head group size and counter ion.

© 2004 Published by Elsevier B.V.

**Keywords:** Micellization; Thermodynamics properties; Quaternary salts; Mass action model; Differential conductivity

## 1. Introduction

Micelle formation of a surfactant in solution is induced by the hydrophobic interaction between hydrocarbon parts of the surfactant molecules balanced by their hydration and electrostatic repulsive effects [1]. Cationic surfactants offer some additional advantages over other class of surfactants [2–5]. These substances besides their surface activity do show antibacterial properties and are used as cationic softeners, lubricants, retarding agents and antistatic agents and in some cases consumer use. Cationic surfactants belonging to quaternary salts are well known compounds and have been examined for their surface and solution behavior using variety of methods [6–15]. The solution properties of cationic surfactants evaluated in terms of critical micelle concentration (CMC), degree of counter ion dissociation ( $\beta$ ), sphere-to-rod transition, aggregation number and thermodynamic quantities are

all simultaneously or synergistically reflected from surfactant ions comprising various combinations of hydrophobic tail with hydrophilic group and from counter ion species.

In aim of this paper was to present the systematic data for quaternary salts as studied by surface tension, electrical conductivity dye solubilization and viscosity measurements. From the CMC values as a function of temperature and considering the mass action model for micelle formation, we have obtained the corresponding thermodynamic parameters of micellization. Aggregation numbers, solubilization power and sphere-to-rod transitions have been evaluated.

## 2. Materials and methods

The cationic surfactants dodecyltrimethylammonium bromide (DTAB), tetradecyltrimethylammonium bromide (TTAB), hexadecyltrimethylammonium bromide (CTAB) and octadecyltrimethylammonium bromide (OTAB), tetradecyltriphenylphosphonium bromide (TTPB), hexadecyltrimethylammonium *p*-toluene sulfonate (CTAT) were Purum grade samples from Lancaster, Leeds, UK. Hexade-

\* Corresponding author. Tel.: +91 261 2258384; fax: +91 261 2256012/2227312.

E-mail addresses: [jitendramata@yahoo.com](mailto:jitendramata@yahoo.com), [jitendramata@sify.com](mailto:jitendramata@sify.com) (J. Mata).

cylpyridinium chloride (CPyC) and hexadecylpyridinium bromide (CPyB) were from Fluka, Switzerland. Hexadecylpyridinium iodide (CPyI) was prepared by the reaction of CPyC and NaI in aqueous solution at ambient temperature where CPyI formed as precipitate was washed several times with water and purified by repeated crystallization from ethanol. Hexadecyltrimethylammonium chloride (CTAC) and dodecylpyridinium chloride (DPyC) were purchased from Aldrich. Dodecylpyridinium bromide (DPyB), tetradecylpyridinium bromide (TPyB), tetradecyl-4-picolinium bromide (TPicB) were prepared by condensation process between respective alkali halide and pyridine/picoline in presence of acetone/ethanol, the product was purified by repeated crystallization from ethanol. Dodecylpyridinium iodide (DPyI) was prepared by the reaction of DPyC and NaI in aqueous solution at ambient temperature where the DPyI formed as precipitate was washed with water and purified from ethanol. Purities of all surfactant samples were ascertained by surface tension measurements; no surface tension concentration plot for any surfactant used in this study showed a minimum. Triple distilled water from an all Pyrex glass apparatus was used for the preparation of solutions for measurements.

### 2.1. Surface tension

The surface tension of surfactant solutions in water was measured by drop weight method using a modified stalagmometer [16]. The assembly consists of Pyrex glass bulb of spherical shape with a capillary tube attached at filling and dropping ends. The capillary tube at the dropping end was blown into a two-fold U shape and the tip of the end was grounded in the form of a fine cone. By this way, not only the formation of drops of uniform shape and size ensured but also drops were allowed to break under their own weight. A thoroughly stoppered weighing bottle was attached to the dropping end through a rubber septum. The weighing bottle attached to a dropping capillary tube was placed suspended in another closed long glass tube. The stalagmometer assembly along with the predried and preweighed weighing bottle was lowered into a thermostatic water bath maintained at the desired temperature (303.15 K) accurate to 0.1 K. A 30 min time of equilibrium was always allowed. Then a known number of drops (>20) of given solution and reference triple distilled water were allowed to fall into the weighing bottle in separate runs. The weight of solutions as well as triple distilled water drawn from separate runs was instantly recorded on single pan balance. The surface tension of the individual solution was then calculated from known values of surface tension of water, densities and weight of solution and water.

### 2.2. Dye solubilization

For dye solubilization experiments, a water insoluble dye, orange OT (1-*o*-tolyl azo-2-naphthol, MW = 262.3) synthesized by coupling of *o*-toluidine and 2-naphthol and recryst-

allized twice from ethanol was used. The dye was shaken with an aqueous solution of the surfactants for 48 h at room temperature and then the residue was removed by means of centrifugation and filtration. The absorbance of the resultant solution was then measured at  $\lambda = 470$  nm using a colorimeter (Erma, Japan).

### 2.3. Conductance

Specific conductivity was measured with a digital conductivity meter (Phillips, India) using a dip-type cell in the temperature range 293.15–333.15 K. The cell constants were determined at different temperatures using KCl solutions. The conductivities were measured at constant temperature while the solutions were diluted successively by adding predetermined amounts of water. All measurements were done in a jacketed vessel, which was maintained at the appropriate temperature ( $\pm 0.1$  K). The errors in the conductance measurements were within  $\pm 0.5\%$ . The conductance was measured after thorough mixing and temperature equilibrium at each dilution. In each experiment, the conductivity of pure water was subtracted from the value indicated by the conductometer.

### 2.4. Viscosity

The viscosity measurements were carried out using an Ubbelohde suspended level capillary viscometer. The viscometer was always suspended vertically in a thermostat with a temperature stability of  $\pm 0.1$  K in the investigated region. The viscometer was cleaned and dried every time before each measurement. The flow time for constant volume of solution through the capillary was measured with a calibrated stopwatch.

## 3. Results and discussion

The surface tension ( $\gamma$ ) of surfactants was measured for a range of concentrations above and below the critical micelle concentration (CMC). A representative plots of  $\gamma$  versus concentration for alkyltrimethylammonium bromide is shown in Fig. 1. A linear decrease in surface tension was observed with increase in surfactant concentrations for all the surfactants up to the CMC, beyond which no considerable change was noticed. This is a common behavior shown by surfactants in solution and is used to determine their purity and CMCs. The CMC data obtained from the break point in the  $\gamma$ -log concentration plots are shown in Table 1. CMC values for all the surfactants are in reasonable agreement with the literature values [17–24]. The  $\gamma$ -log concentration plots also provides information about area per molecule at air–water interface, effectiveness and efficiency of the surfactants.

The surface excess concentration of surfactant ions  $\Gamma_s$  and the area per molecule was calculated from the slope of the straight line in the surface tension plot ( $d\gamma/d \ln C$ )

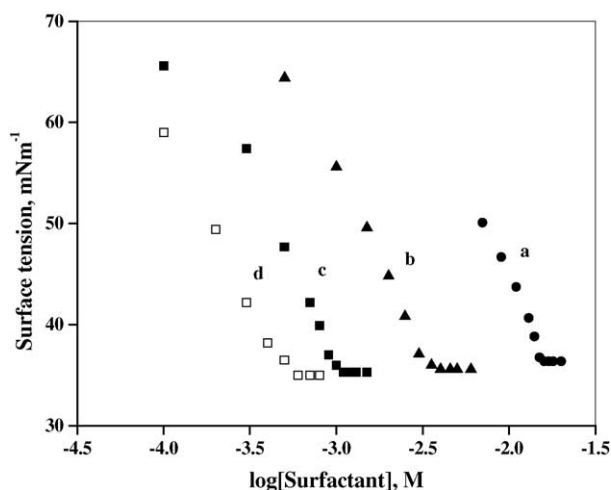


Fig. 1. Surface active behavior of different surfactants in water at 303.15 K: (a) DTAB, (b) TTAB, (c) CTAB and (d) OTAB.

below CMC, using appropriate form of Gibbs adsorption equation

$$\Gamma_s = -\frac{1}{nRT} \left( \frac{d\gamma}{d \ln C} \right) \quad (1)$$

The values of area per molecule obtained are shown in Table 1, which shows good agreement with the reported value [17,25]. For cationic surfactants with same head group area but different chain length or counter ion, the area values remain more or less same. Since the area per molecule at the interface is primarily influenced by head group size, a large value of area per molecule for TPPB as compared to TTAB can be anticipated. Efficiency and effectiveness increases with lengthening the alkyl chain and the strong binding ability of the counter ion. When the logarithms of CMC of surfactant homolog at constant temperature are plotted against the number of carbon atoms in the alkyl chain, they often give linear plots. Such plots for alkytrimethylammonium bromide

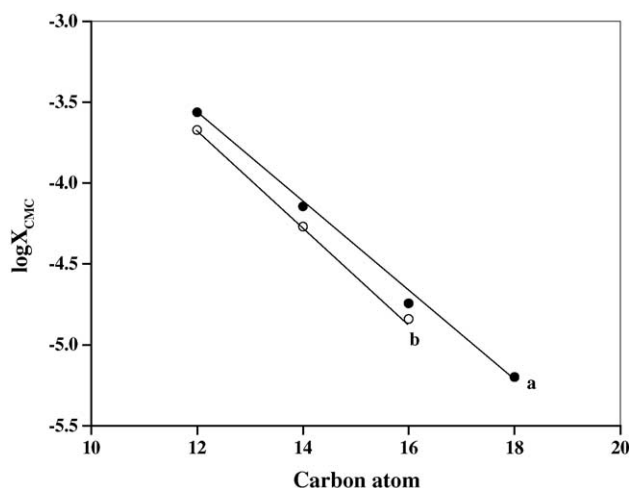


Fig. 2. Plot of logarithm of critical micelle concentration (from surface tension) in mole fraction of *n*-alkyltrimethylammonium bromide and alkylpyridinium bromide as a function of the number of alkyl chain carbon atoms in water at 303.15 K.

and alkylpyridinium bromide are shown in Fig. 2 and the experimental data show a linear dependence.

Solubilizing power is one of the most important properties of surfactants. There are a few methods known by which CMC of surfactants can be experimentally determined through the use of solubilization measurements. A number of approaches have been taken to measure solubilizing behavior of surfactants. One of these is a colorimetric method in which the solubilization of water insoluble dye orange OT in the surfactant micelles was studied in order to determine the CMC of the surfactants. The obtained results were plotted as absorbance versus concentration of the surfactants. Solubilization plots (Fig. 3) reveal that the amount of the dye solubilized was little up to the CMC of each surfactant and thereafter a sudden and steep rise was observed with the formation of micelles in the bulk. The CMC value for each surfactant obtained by this method (Table 1) is in good agree-

Table 1  
Interfacial properties of cationic surfactants in water at 303.15 K

Surfactants	CMC (mM)			$C_{\pi=20}$ (mM)	$\gamma_{\text{CMC}}$ (mN m <sup>-1</sup> )	Area/molecule (Å <sup>2</sup> )	
	$\gamma$	DS	Literature			Experimental	Literature
DPyC	17.50	17.40	17.00 [13]	7.80	35.8	52.5	–
DPyB	11.85	11.72	10.00 [8]	4.15	35.6	51.8	–
DPyI	5.30	5.28	–	1.02	35.0	51.6	–
DTAB	15.20	15.10	15.00 [17]	6.50	36.4	50.0	49.0 [17]
TPyB	2.98	2.92	2.65 [18]	1.25	34.9	53.0	41.0 [18]
TTAB	3.98	3.90	3.83 [19]	1.70	35.6	51.1	–
TTPB	0.60	0.59	0.71 [20]	0.20	41.3	82.2	–
TPicB	2.59	2.50	–	1.10	33.1	58.1	–
CPyC	0.91	0.88	1.00 [23]	0.5	42.0	42.0	–
CPyB	0.80	0.78	0.82 [24]	0.2	34.8	41.0	–
CTAC	1.30	1.25	1.30 [22]	0.80	41.0	54.0	–
CTAB	1.00	0.98	1.00 [19]	0.40	35.3	51.7	48.5 [25]
CTAT	0.23	0.22	0.20 [22]	0.08	32.0	48.1	63.0 [22]
OTAB	0.35	0.33	0.34 [21]	0.15	35.0	51.9	–

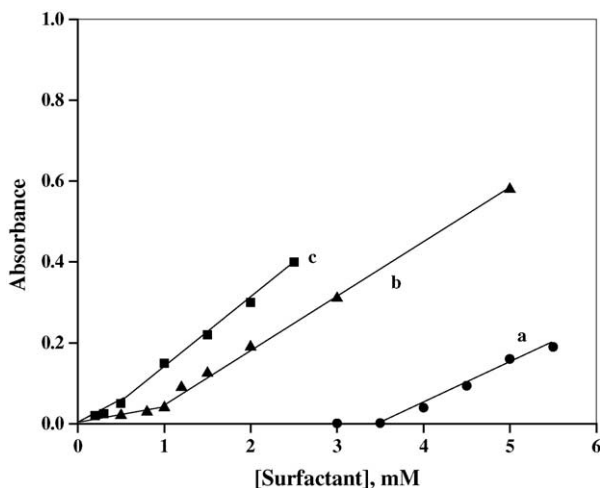


Fig. 3. UV-visible absorbance of orange OT as function of surfactants concentration: (a) TTAB, (b) CTAB and (c) OTAB.

ment with the CMC determined by surface tension method. Mukerjee and Mysels [21] concluded that the presence of a solubilized indicator always lowers the CMC and this lowering reaches a maximum if the micelle is saturated with the indicator during the determination. Since the solubility of orange OT is very small in the surfactant solutions we have examined, the lowering of CMC is negligible.

Conductivity measurements were performed for cationic surfactants at various temperatures (293.15–333.15 K) in order to evaluate the CMC and the degree of counter ion dissociation,  $\beta$ . It is known that the specific conductivity is linearly correlated to the surfactant concentration in both the pre-micellar and in the postmicellar regions, being the slope in the pre-micellar region greater than that in the postmicellar region [20]. The intersection point between the two straight lines gives the CMC while the ratio between the slopes of the postmicellar region to that in the pre-micellar region gives counter ion dissociation,  $\beta$ . Representative plots of conductance data for solutions of DPyB in water at various temperatures are presented as specific conductance versus concentration plots in Fig. 4 and molar conductance versus square root of concentration plots in Fig. 5. However, as the temperature increases, we found that a smaller curvature appeared around the CMC; consequently the CMC and  $\beta$  values obtained are affected to a greater uncertainty. Therefore we decided to use a new approach that has recently been applied successfully in a determination of precise values of the CMC [26]. This approach is based on the analysis of the plots of differential conductivity, which will henceforth be written as  $dk/dc$ , versus the total surfactant concentration. Example of this plot is shown in Fig. 6. It can be seen that the curve shows an abrupt fall, having a reverse sigmoid. This procedure enables us to determine the CMC values more precisely than the conventional method. The CMC value is given by the centre of the sigmoid and can be obtained from fitting the data to a sigmoid. The values of CMC and  $\beta$  at various temperatures for all the cationic surfactants are shown in Table 2.

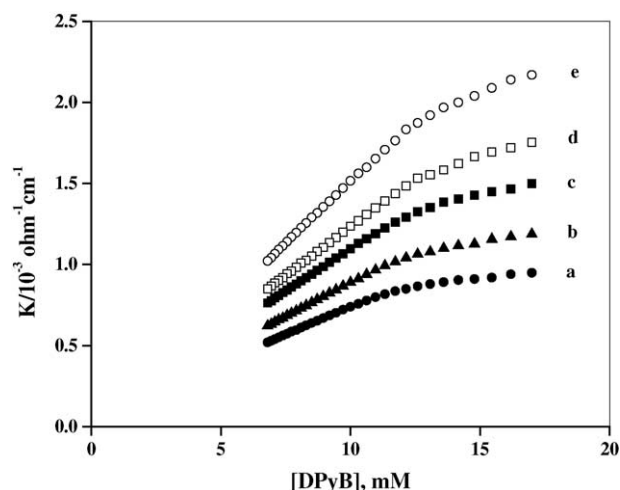


Fig. 4. Plots of specific conductivity vs. concentration of DPyB in water at different temperatures: (a) 293.15 K, (b) 303.15 K, (c) 313.15 K, (d) 323.15 K and (e) 333.15 K.

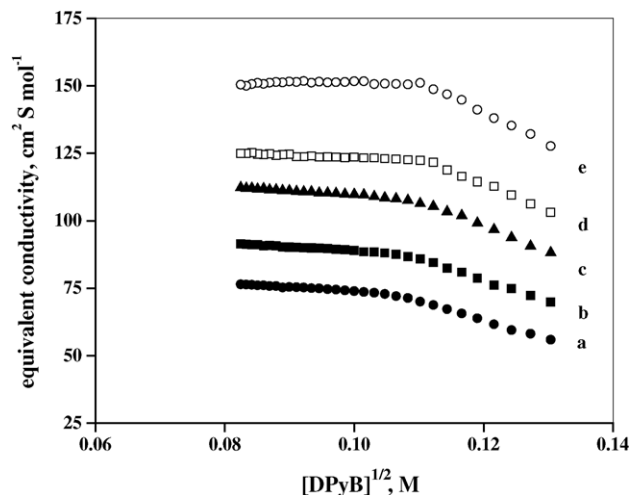


Fig. 5. Plots of equivalent conductivity vs. square root of concentration of DPyB in water at different temperatures: (a) 293.15 K, (b) 303.15 K, (c) 313.15 K, (d) 323.15 K and (e) 333.15 K.

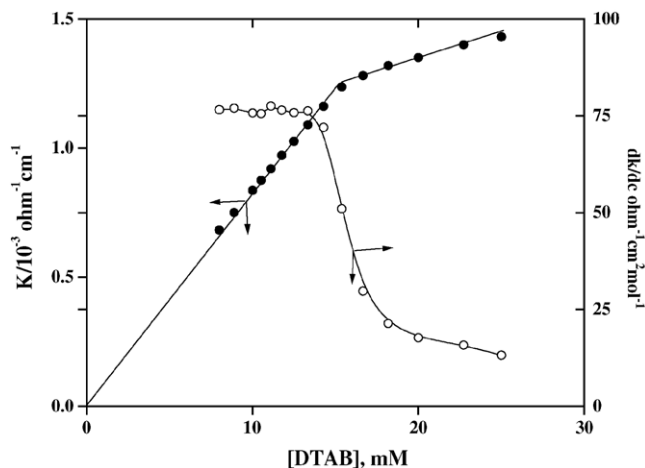


Fig. 6. Specific conductivity ( $k$ ) and differential conductivity ( $dk/dc$ ) vs. total concentration of DTAB at 293.15 K.

Table 2

The CMCs, degree of counter ion dissociation ( $\beta$ ), standard molar gibbs energies, enthalpies and entropies of micellization, equivalent conductivity of the solute at infinite dilution ( $\Lambda_0$ ) and aggregation number ( $N_{\text{agg}}$ ) for cationic surfactants in water at different temperatures

Temperature (K)	CMC (mM)	$\beta$	$\Delta G_m^0$ (kJ mol <sup>-1</sup> )	$\Delta H_m^0$ (kJ mol <sup>-1</sup> )	$\Delta S_m^0$ (kJ mol <sup>-1</sup> )	$\Lambda_0$ (cm <sup>2</sup> Ω <sup>-1</sup> mol <sup>-1</sup> )	$N_{\text{agg}}$
<b>DPyC</b>							
293.15	16.67	0.371	-5.44	-0.94	0.016	84.3	44
303.15	17.70	0.420	-5.46	-1.35	0.014	111.2	43
313.15	17.88	0.509	-5.48	-1.36	0.013	127.8	41
323.15	18.10	0.521	-5.58	-1.43	0.013	138.3	38
333.15	18.52	0.527	-5.66	-1.52	0.012	151.1	37
<b>DPyB</b>							
293.15	11.70	0.256	-7.33	-1.90	0.019	85.4	58
303.15	11.85	0.315	-7.38	-2.11	0.017	105.1	56
313.15	12.20	0.336	-7.43	-2.23	0.017	125.3	53
323.15	12.40	0.366	-7.47	-2.33	0.016	136.5	50
333.15	12.60	0.406	-7.49	-2.42	0.015	150.8	48
<b>DPyI</b>							
293.15	5.16	0.215	-10.72	-6.46	0.015	108.4	77
303.15	5.51	0.248	-10.62	-6.39	0.014	145.2	76
313.15	6.00	0.273	-10.47	-6.33	0.013	159.8	75
323.15	6.30	0.406	-9.78	-6.22	0.011	179.0	72
333.15	6.40	0.429	-9.88	-6.52	0.010	195.1	70
<b>DTAB</b>							
293.15	15.38	0.222	-6.52	-2.64	0.014	111.1	58
303.15	15.63	0.278	-6.58	-2.73	0.013	134.0	54
313.15	16.12	0.281	-6.68	-2.91	0.012	147.0	51
323.15	16.64	0.292	-6.73	-3.08	0.011	158.5	49
333.15	16.70	0.302	-6.80	-3.15	0.009	162.1	47
<b>TPyB</b>							
293.15	2.9	0.251	-12.80	-2.62	0.035	120.2	86
303.15	3.0	0.272	-12.90	-2.74	0.034	137.9	81
313.15	3.2	0.294	-12.92	-2.88	0.032	154.4	72
323.15	3.3	0.339	-12.95	-2.99	0.031	177.2	69
333.15	3.5	0.342	-12.98	-3.12	0.029	182.0	62
<b>TTAB</b>							
293.15	3.53	0.238	-12.10	-8.84	0.011	102.2	81
303.15	3.75	0.239	-12.25	-9.45	0.009	122.5	76
313.15	4.00	0.241	-12.37	-10.08	0.007	140.0	72
323.15	4.44	0.276	-12.46	-10.52	0.005	159.5	67
333.15	4.60	0.282	-12.55	-11.00	0.002	169.1	60
<b>TTPB</b>							
293.15	0.75	0.479	-16.28	-19.73	-0.012	103.1	40
303.15	0.83	0.499	-15.96	-20.13	-0.014	122.0	38
313.15	0.88	0.554	-15.41	-20.04	-0.015	141.2	35
323.15	0.99	0.586	-14.89	-20.24	-0.017	151.0	34
333.15	1.08	0.602	-14.00	-19.20	-0.019	158.1	30
<b>TPicB</b>							
293.15	2.55	0.350	-12.82	-9.01	0.015	114.2	52
303.15	2.67	0.360	-12.74	-9.20	0.012	116.0	49
313.15	3.00	0.372	-12.59	-9.74	0.009	120.2	41
323.15	3.15	0.399	-12.58	-10.20	0.007	131.1	38
333.15	3.40	0.428	-12.42	-10.65	0.005	145.3	30
<b>CPyC</b>							
293.15	1.02	0.371	-15.74	-9.05	0.024	142.3	82
303.15	1.11	0.396	-15.80	-9.53	0.021	150.0	79
313.15	1.18	0.448	-15.85	-9.84	0.019	162.4	71
323.15	1.25	0.450	-15.90	-10.46	0.017	183.5	64
333.15	1.43	0.489	-15.92	-10.84	0.014	201.5	59
<b>CPyB</b>							
293.15	-	-	-	-	-	-	-
303.15	0.71	0.232	-19.16	-8.04	0.038	140.2	111
313.15	0.77	0.281	-19.22	-8.33	0.035	159.5	106
323.15	0.83	0.294	-19.32	-8.81	0.033	182.2	99
333.15	0.85	0.340	-19.38	-9.11	0.031	208.0	90

Table 2 (Continued)

Temperature (K)	CMC (mM)	$\beta$	$\Delta G_m^0$ (kJ mol <sup>-1</sup> )	$\Delta H_m^0$ (kJ mol <sup>-1</sup> )	$\Delta S_m^0$ (kJ mol <sup>-1</sup> )	$\Lambda_0$ (cm <sup>2</sup> Ω <sup>-1</sup> mol <sup>-1</sup> )	$N_{agg}$
<b>CPyI</b>							
293.15	–	–	–	–	–	–	–
303.15	–	–	–	–	–	–	–
313.15	0.48	0.222	–22.04	–11.07	0.035	181.8	110
323.15	0.50	0.274	–21.89	–11.45	0.032	225.6	105
333.15	0.56	0.316	–21.50	–11.87	0.029	262.4	96
<b>CTAC</b>							
293.15	1.35	0.402	–14.59	–5.09	0.032	102	88
303.15	1.40	0.425	–14.76	–5.37	0.030	110	83
313.15	1.46	0.468	–14.69	–5.58	0.029	122	80
323.15	1.55	0.510	–14.44	–5.75	0.027	133	77
333.15	1.62	0.525	–14.25	–5.90	0.025	140	72
<b>CTAB</b>							
293.15	–	–	–	–	–	–	–
303.15	0.91	0.290	–17.80	–9.26	0.028	128.0	98
313.15	0.10	0.291	–17.87	–9.87	0.026	152.1	92
323.15	1.05	0.364	–17.93	–10.06	0.023	169.0	86
333.15	1.12	0.385	–17.95	–10.35	0.019	178.3	81
<b>CTAT</b>							
293.15	0.22	0.194	–24.42	–15.98	0.029	130	105
303.15	0.24	0.212	–24.58	–16.90	0.025	142	102
313.15	0.27	0.255	–24.29	–17.63	0.021	158	98
323.15	0.32	0.286	–23.85	–18.46	0.017	179	92
333.15	0.35	0.301	–23.99	–19.00	0.015	190	85
<b>OTAB</b>							
293.15	–	–	–	–	–	–	–
303.15	0.39	0.257	–21.77	–5.01	0.055	138.2	180
313.15	0.42	0.283	–21.91	–5.26	0.053	159.6	172
323.15	0.43	0.293	–22.38	–5.57	0.052	178.0	161
333.15	0.44	0.312	–22.45	–5.65	0.050	185.1	149

Minimum in CMC at certain temperature,  $T_{min}$ , was not observed for any surfactant in the temperature range studied. Actually the  $T_{min}$  shifts towards a lower temperature as the alkyl chain of the surfactant becomes longer. We could not see  $T_{min}$  for such surfactant, since 293.15 K is the initial temperature of our experimental studies.

A comparison of CMC for homologous series of surfactant demonstrates that increasing the length of the hydrocarbon chain has the tendency of lowering the concentration at which aggregation is initiated, owing to enhanced hydrophobic interaction between the counter ion and micellar core. Increasing the length of the hydrocarbon chain increases the average micellar aggregation number and shifts the krafft discontinuity to higher temperature [27]. The CMC of identical chain length surfactant with bromide counter ion is less as compared to that with chloride counter ion. The chloride and bromide ions have different sizes in solution [25] and the average number of bound water molecules for the bromide ion is less in comparison to chloride ion. Therefore, the hydrated chloride ion is larger than the hydrated bromide ion and as such the chloride ion is not as closely associated with the cationic head group of the surfactant and will not be as effective as the bromide counter ion at neutralizing the head group charge. This will lead to a greater electrostatic repulsion between the head group of the surfactants not only within the micellar aggregates but also between the surfactant aggregates themselves. The lower value of CMC in case of

CTAT is due to the higher degree of binding of tosylate ion as compared to bromide and chloride ion.

In case of TTAB, TTPB, TPyB and TPicB despite of having very bulky polar head group, TTPB has quite low value of CMC as compared to TTAB, which can be explained on the basis that the presence of three phenyl groups in the polar head group region of TTPB may impart additional hydrophobicity that helps it to undergo micelle formation more favorably [20]. Similar explanation can be provided for TPicB having higher CMC as compared to TPyB.

The plot of specific conductivity versus concentration at gradual increase in temperature indicates that the CMC increases with temperature in the range investigated. The effect of temperature on the CMC of surfactants in aqueous solution is usually analyzed in terms of two opposing factors. First, as the temperature increases the degree of hydration of the hydrophilic group decreases, which favors micellization, however, an increase in temperature also causes the disruption of the water structure surrounding the hydrophobic group and this is unfavorable to micellization. It seems from the data in Table 2, that this second effect is predominant in the temperature range studied. On the other hand, the degree of counter ion dissociation in the surfactant micelles,  $\beta$ , also increases regularly with temperature increase. This observed increase in  $\beta$  is probably due to a decrease in the charge density at the micellar surface caused by the decrease in the aggregation number of the micelle.



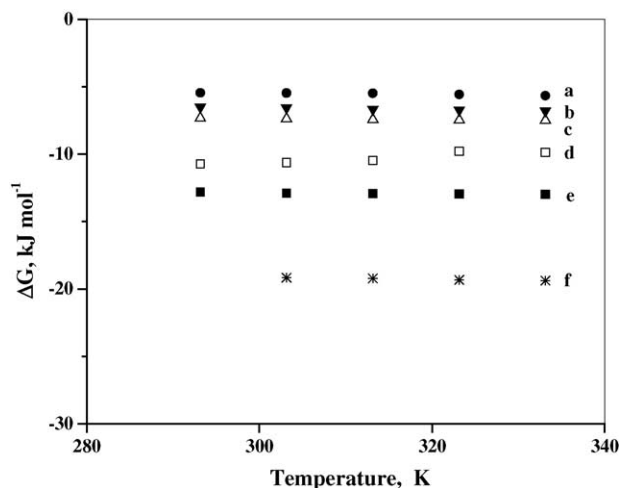


Fig. 7. Plots of standard free energy of micelle formation of different surfactants in aqueous solutions at several temperatures: (a) DPyC, (b) DTAB, (c) DPyB, (d) DPyI, (e) TPyB and (f) CPyB.

The CMC of a surfactant is regarded as a measure of the stability of its micellar form relative to its monomeric form. Lower the CMC, greater the stability. In the charged pseudo-phase model of micelle formation, the standard free energy of micelle formation per mole of surfactant is given by

$$\Delta G_m^\circ = (2 - \beta)RT \ln X_{\text{CMC}} \quad (2)$$

where  $R$  is the gas constant,  $T$  the temperature and  $X_{\text{CMC}}$  stands for the CMC in the mole fraction unit.

Fig. 7 shows the relationship between the standard free energy of micelle formation of alkyltrimethylammonium bromide and temperature. The free energy decreases with rising temperature. This decrease is caused by the effect of the coefficient  $RT$  in Eq. (2), together with the negative value of the  $\ln X_{\text{CMC}}$ , rather than by the small temperature change of the CMC. The negative slope corresponds to the positive value of standard entropy of micelle formation, which indicates that micelle formation is favored entropically.

The standard enthalpy of micelle formation ( $\Delta H_m^\circ$ ) can be derived by the van't Hoff equation

$$\Delta H_m^\circ = -(2 - \beta)RT^2 \left[ \left( \frac{\partial \ln X_{\text{CMC}}}{\partial T} \right) \right] \quad (3)$$

One can see that the standard enthalpy of micelle formation is more negative or exothermic on higher temperature side. Therefore, the enthalpy of micellization may be obtained if the dependence of the CMC on temperature is known. The slope in the plot of  $\ln X_{\text{CMC}}$  against  $T$  at each temperature was taken as  $[(\partial \ln X_{\text{CMC}})/\partial T]$ . A linear plot was observed for both the surfactants as shown in Fig. 8. The standard entropy of micelle formation entropic ( $\Delta S_m^\circ$ ) was calculated from

$$\Delta S_m^\circ = \left[ \frac{\Delta H_m^\circ - \Delta G_m^\circ}{T} \right] \quad (4)$$

The entropy change is positive in all cases. However it decreases with increasing temperature. The thermodynamic pa-

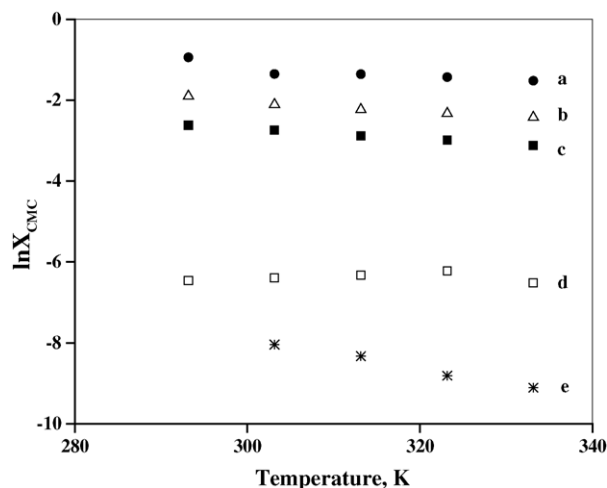


Fig. 8. Plots of  $\ln X_{\text{CMC}}$  vs. temperature for different surfactants in water: (a) DPyC, (b) DPyB, (c) TPyB, (d) DPyI and (e) CPyB.

rameters of micellization obtained by following the above procedure are listed in Table 2.

We have used the conductivity data obtained for the low concentration range of cationic surfactant to estimate, by extrapolation, the equivalent conductivity of the solute at infinite dilution,  $\Lambda_0$ . An estimation of the micellar charge from conductivity data of aqueous surfactant solutions can be made by applying the approach of Kimizuka and Satake [28], they assumed that above the CMC there is only one kind of micelle aggregation number  $n$ , with a degree of ionization amounting to  $\beta$ . An additional assumption that  $\Lambda = \Lambda_0 + a\sqrt{I}$  (where  $a$  is a constant and  $I$  the ionic strength) is valid in the pre- and postmicellar regions and leads to the equation

$$\left( \frac{\Lambda_0 - \Lambda}{\Lambda_0 - \Lambda_{\text{CMC}}} \right)^2 = 1 - \frac{\beta(1 + n\beta)}{2} + \frac{\beta(1 + n\beta)}{2} \left( \frac{C}{C_{\text{CMC}}} \right) \quad (5)$$

where  $\Lambda_{\text{CMC}}$  is the equivalent conductivity of the solute just at the CMC. From the linear relation between  $[(\Lambda_0 - \Lambda)/\Lambda_0 - \Lambda_{\text{CMC}}]^2$  and  $C/C_{\text{CMC}}$ , the value of aggregation number  $n$  can be inferred. The value of  $n$  can be obtained either from the intercept or from the slope. Both approaches yield comparable values of  $n$ , which are matches with literature values.

We have used viscosity measurements to obtain the concentration at which the sphere-to-rod transitions of the micelles of various cationic surfactants occur. Representative plots of relative viscosities of surfactant solutions at different concentrations of alkyltrimethylammonium bromides (DTAB, TTAB, CTAB and OTAB) of varying chain length were examined at 303.15 K and the results obtained are shown in Fig. 9. All the measurements were made above the CMC for each surfactant. The relative viscosity increases gradually with concentration but the increase is more pronounced in case of surfactant with longer chain length. Increasing the hydrocarbon chain of surfactant has qualitatively similar ef-

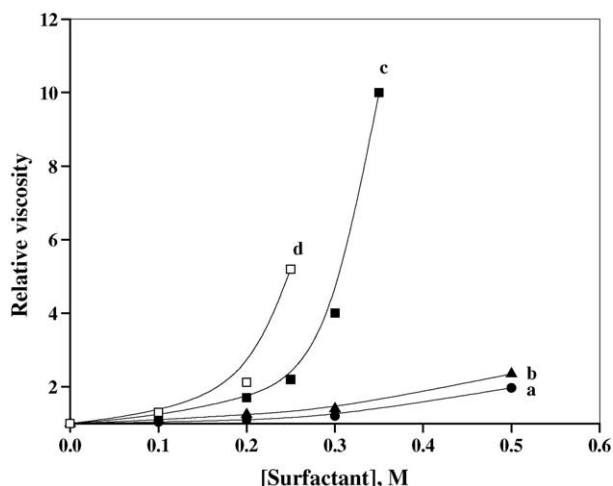


Fig. 9. Relative viscosity vs. concentration of different surfactants at 303.15 K: (a) DTAB, (b) TTAB, (c) CTAB and (d) OTAB.

fects to increasing the surfactant concentration on micellar properties, thus increasing the amount of nonpolar material in the system will result in an increase in micellar size due to hydrophobic interaction between the hydrocarbon tails and the aqueous solvent molecules. Hence, we can say that if the hydrocarbon part is longer, the surfactant is adapted to rodlike micelle better than to a spherical micelle, which is well reflected from our viscosity results. An exceptionally rapid increase in viscosity in case of OTAB and CTAB suggests a formation of rodlike micelle at much lower concentration as compared to other homologues with shorter hydrocarbon chain.

Hexadecyltrimethylammonium salts are well known for the formation of rodlike (or wormlike) micelles, but the concentration at which the formation of these rodlike micelles initiates depends upon the nature of counter ion attached. One of the counter ions that are able to induce the formation of rodlike micelles from hexadecyltrimethylammonium surfactants at a very low concentration is tosylate. Gamboa and Sepulveda [29] first introduced CTAT for the measurement of the degree of dissociation of CTAX, in which X represents inorganic counter ions. The globular micelles of CTAT are initially formed above the CMC. These micelles start to grow at a concentration of around 15–20 mM, which could be due to their ability to form large rodlike micelles by virtue of their bulky tosylate counter ions with a high degree of binding. Sphere-to-rod transitions in CTAB occur at much higher concentration (0.25–0.3 M) compared to CTAT (15–20 mM) while CTAC does not show such a behavior and the aggregates remaining globular upto 0.7 M. This difference in concentration for the transition could be considered to stand for the stronger binding of tosylate as compared to  $\text{Br}^-$  and  $\text{Cl}^-$  to the cationic micelle. The counter ion thus plays a very important role in micelle formation and geometry. Similar explanation can be provided for other surfactants.

#### 4. Conclusions

The physicochemical properties of the quaternary salt-based cationic surfactants in aqueous solution have been investigated by means of surface tension, conductance, dye solubilization and viscosity measurements. Aggregation numbers estimated by using the procedure suggested by Kimizuka and Satake [28] and the thermodynamic of micellization are the main contributions of this work. Other aspects as power of solubilization and the presence of sphere-to-rod transitions have been shown as a function of the surfactant concentration. From these results it appears that changes in the nature of the surfactant (such as changes in chain length, polar head group or counter ion) have a severe effect on the subsequent self-assembly in water. The increase in hydrophobic character of the surfactant decreases the CMC, induces sphere-to-rod transition at lower concentration and increases the solubilizing power of surfactant towards orange OT. Viscosity results indicated that the size of the micelles is relatively small at CMC and grows longer with increasing surfactant concentration. The plots of differential conductivity,  $(dk/dc)_{T,P}$ , versus the total surfactant concentration enables us to determine the CMC values more precisely.

#### References

- [1] C. Tanford, *The Hydrophobic Effect-Formation of Micelles and Biological Membranes*, 2nd ed., Wiley, New York, 1980.
- [2] E. Jungerman, *Cationic Surfactants*, Marcel Dekker, New York, 1969.
- [3] J. Cross, E.J. Singer, *Cationic Surfactants: Analytical and Biological Evaluation*, Marcel Dekker, New York, 1994.
- [4] P.M. Holland, D.N. Rubingh (Eds.), *Cationic Surfactants: Physical Chemistry*, Marcel Dekker, New York, 1991.
- [5] J.M. Richmond, *Cationic Surfactants: Organic Chemistry*, Marcel Dekker, New York, 1990.
- [6] Z. Adamczyk, G. Para, P. Warszynski, *Langmuir* 15 (1999) 8383–8387.
- [7] M.S. Bakshi, *Colloid Polym. Sci.* 278 (2000) 1155–1163.
- [8] J. Skerjanc, K. Kogej, J. Cerar, *Langmuir* 15 (1999) 5023–5028.
- [9] J.M. Ruso, F. Sarmiento, *Colloid Polym. Sci.* 278 (2000) 800–804.
- [10] R. Zielinski, *J. Colloid Interface Sci.* 235 (2001) 201–209.
- [11] R. Ranganathan, L.T. Okano, C. Yihwa, F.H. Quina, *J. Colloid Interface Sci.* 214 (1999) 238–242.
- [12] K. Fujio, T. Mitsui, H. Kurumizawa, Y. Tanaka, Y. Uzu, *Colloid Polym. Sci.* 282 (2004) 223–229.
- [13] J.J. Galan, A. Gonzalez-Perez, J.L. Del Castillo, J.R. Rodriguez, *J. Therm. Anal. Calcd.* 70 (2002) 229–234.
- [14] O.R. Pal, V.G. Gaikar, J.V. Joshi, P.S. Goyal, V.K. Aswal, *Langmuir* 18 (2002) 6764–6768.
- [15] J.M. Ruso, D. Attwood, P. Taboada, V. Mosquera, *Colloid Polym. Sci.* 280 (2002) 336–341.
- [16] S.S. Soni, N.V. Sastry, V.K. Aswal, P.S. Goyal, *J. Phys. Chem.* 106 (2002) 2607–2617.
- [17] K.M. McGrath, *Langmuir* 11 (1995) 1835–1839.
- [18] K. Fujio, *Bull. Chem. Soc. Jpn.* 71 (1998) 83–89.
- [19] C. Carnero Ruiz, J. Aguiar, *Langmuir* 16 (2000) 7946–7953.
- [20] M.S. Bakshi, *J. Colloid Interface Sci.* 227 (2000) 78–83.
- [21] P. Mukerjee, K.J. Mysels, *Critical Micelle Concentrations of Aqueous Surfactant Systems*, NSRDC-NBS-36, Washington, DC, 1971.
- [22] C. Gamboa, H. Rios, V. Sanchez, *Langmuir* 10 (1994) 2025–2027.



- [23] M.S. Bakshi, S. Mahajan, *J. Jpn. Oil Chem. Soc.* 49 (2000) 17–24.
- [24] M.S. Bakshi, G. Kaur, *J. Surf. Deterg.* 3 (2000) 159–166.
- [25] M. Bhat, V.G. Gaikar, *Langmuir* 15 (1999) 4740–4751.
- [26] C. Carnero Ruiz, *Colloid Polym. Sci.* 277 (1999) 701–707.
- [27] D.M. Small, *The Physical Chemistry of Lipids: From Alkanes to Phospholipids*, vol. 4, Plenum Press, New York, 1986.
- [28] H. Kimizuka, I. Satake, *Bull. Chem. Soc. Jpn.* 35 (1962) 251.
- [29] C. Gamboa, L. Sepulveda, *J. Phys. Chem.* 93 (1989) 5540–5543.